The 2013 World Congress on
Advances in Structural Engineering and Mechanics (ASEM13)
Jeju, Korea, September 8-12, 2013

Micromechanics-based elasticity prediction of hardened cement paste

*Jun Chen[1)] and Xianyu Jin[2)]

[1), 2)] *Department of Civil Engineering and Architecture, Zhejiang University, Hangzhou,China*
[1)] chenchangejun@zju.edu.cn

ABSTRACT

A *Composite-Equivalent Inclusions Model (CEI Model)* was established for micromechanics-based elasticity prediction of hardened cement paste and compared with previous matrix-inclusion type and polycrystalline type models. It was found that pure matrix-inclusion type or polycrystalline type models would overestimate or underestimate the elasticity of hardened cement paste when w/c was above 0.5. Polycrystalline type model might excel matrix-inclusion type model in represent ability for hardened cement paste when w/c decreased from 0.4.The morphological effect of inclusions had a significant influence on prediction results when solid volume fraction was lower than 79%.The imperfect bond between crystalline hydrates and matrix began to exert impact when the porosity of cement paste increased from 0.21, and the newly proposed *CEI model* provided an effective approach to solve this problem by dividing micro CH into two groups. It could accurately predict the elasticity value of hardened cement paste with w/c ranging from 0.5 to 0.9 with an average error of 4.3%.

1. INTRODUCTION

Elasticity prediction of hardened cement paste from micron or even finer scale has been realized for years with the development of nanoindentation technique and the application of classical micromechanics theory. However, the chosen representative volume element (RVE) for hardened cement paste differed from one author to another. The most applied RVE by now was matrix-inclusion type (Bernard et al 2003; Constantinides and Ulm 2004) or polycrystalline type (Pichler et al 2009; Pichler and Helllmich 2011) with less account of morphological effect and imperfect interfacial impact. In this paper, the present two types of representative RVE were evaluated and discussed, and a new RVE was built and applied for hardened cement paste with larger porosity when imperfect interface has a notable impact.

[1)] Graduate Student

[2)] Professor

2. Verification of Polycrystalline type and Matrix-inclusion type RVEs

To mechanically represent the microstructure of hardened cement paste, two main forms of RVEs had been proposed.

Matrix-inclusion type: Constantinides and Ulm's Model (2004) represented cement paste as a matrix-inclusion type composite: HD C-S-H as spherical inclusions embedded in LD C-S-H matrix at Level Ⅰ; homogenized C-S-H matrix to embed three types of spherical inclusions (CH, air voids, and unhydrated clinkers) at Level Ⅱ. *Zheng's Model (2010)* developed a simple three-step analytical scheme for elasticity prediction of hardened cement paste. At Step 1, the outer hydrates (CH and LD C-S-H) and the inner hydrates (CH and HD C-S-H) were both modeled as a two-phase composite sphere, in which CH is the inclusion phase with constant volume fraction; At Step 2, the solid cement paste was modeled as a three-phase composite in which the outer hydrates act as the matrix while the inner hydrates and unhydrated clinkers act as equivalent inclusion phase; At Step 3, the hardened cement paste was modeled as capillary pores dispersed in the solid cement paste.

Polycrystalline type: Pichler's Model (2011) represented cement paste as a four-phase polycrystalline composite built up of clinkers, hydrates, water and air. However, the mechanical constant of LD C-S-H was chosen as representative for all the hydration products for the sake of simplicity. Thus, two modified forms of *Pichler's Model* with the consideration of mechanical variance of hydrates were applied in this paper (see Fig.1).

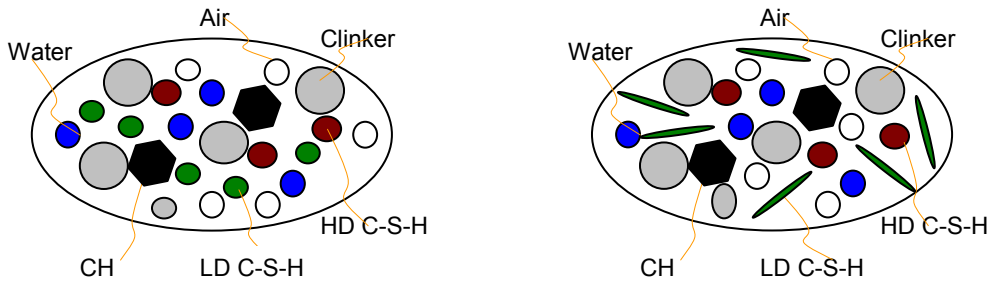

(a) Spherical LD C-S-H (b) Acicular LD C-S-H

Fig. 1 Modified *Pichler's Model*

Fig. 2 was the verification of matrix-inclusion type and polycrystalline type RVEs by experimental data from Helmuth and Turk (1966), in which one C_3S paste and two types of Portland cement paste aged from 6 to 24 months had been tested.

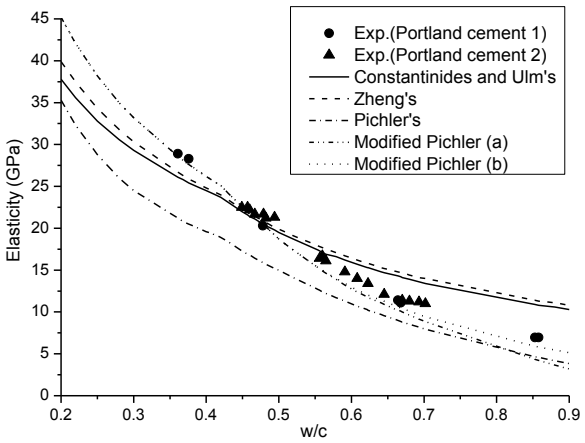

Fig. 2 Elasticity prediction of hardened cement paste by matrix-inclusion type and polycrystalline type RVEs

As Fig. 2 depicted, for matrix-inclusion type RVEs, *Constantinides and Ulm's Model* and *Zheng's Model* predicted a similar curve of elasticity versus w/c with an average prediction error of 15.0% and 17.3% respectively. It was revealed that matrix-inclusion type RVEs might overestimate or underestimate the elasticity value of hardened cement paste when w/c was above 0.5 or below 0.4. Comparison between *Pichler's Model* and the two Modified *Pichler's Models* effectively proved that the simplification taken in *Pichler's Model* greatly undermined the predict ability of polycrystalline type RVEs. It can be learned from Fig. 2 that polycrystalline type RVEs (*Modified Pichler's Models*) generally predicted a more accurate value than matrix-inclusion type RVEs, especially for hardened cement paste with lower w/c. The predictive curve of *Modified Pichler's Models (a)* and *(b)* nearly overlapped each other until w/c increased from about 0.55 (with porosity at about 21%), which indicated that the morphological effect of inclusions had a negligible influence on prediction results when solid volume fraction was greater than about 79%. It should be noted that neither matrix-inclusion type nor polycrystalline type RVEs could successfully predict elasticity of hardened cement paste when w/c was above 0.5, under which condition cement paste owns a more porous microstructure.

3. A *Composite-Equivalent Inclusions Model* for hardened cement paste

Verification results in Fig. 2 demonstrated the limitation of the present matrix-inclusion type and polycrystalline type RVEs in mechanically representing hardened cement paste. Thus, an improvement in RVE for hardened cement paste is highly desirable. Fig.3 was one microstructural graph of hardened cement paste whose w/c was 0.53 taken by ESEM. The gel hydrates, aluminates and CH crystals could be identified in the picture. According to their precipitation location, these hydration products could be classified into two groups. One refers to the C-S-H gels which grow closely around cement particles (Garrault et al. 2005; Scrivener 2004) and binds them

together to form continuous matrix. The other are crystalline hydrates (CH and aluminates), which precipitate preferentially inside free space in capillary pores (Scrivener 2004; Diamond 2004). It was clear that there are voids and gaps between the crystalline hydrates and matrix, which might disappeared only when the capillary porosity decreased to an extremely low level. Thus, modeling the crystalline hydrates as perfect inclusions (as in the aforementioned matrix-inclusion type RVEs) would overestimate the elasticity of hardened cement paste. Besides, polycrystalline type RVE might also not be suitable for hardened cement paste with higher w/c, as LD C-S-H took a considerable volume fraction in this case (Constantinides and Ulm 2007) and granted the paste a definite matrix-inclusion feature. In view of this, a new RVE considering the imperfect bond between matrix and inclusions for hardened cement paste was proposed here. As Fig. 4 depicted, three types of inclusions were considered in the new RVE: 1) Composite Inclusion: separated crystalline hydrates (a type CH and aluminates) with voids and water in-between; 2) Equivalent Inclusion: Unhydrated clinker surrounded by HD C-S-H; 3) Individual inclusions: b type CH plates and AFt rods fully embedded in the matrix. The elastic moduli of each individual hydrates were obtained from the literature (Acker 2001; Constantinides and Ulm 2004; Monteiro and Chang 1995). Aluminates phases were neglected to accord with previous matrix-inclusion type and polycrystalline type RVEs. This new RVE was denoted as *Composite-Equivalent Inclusions Model (CEI Model)*.

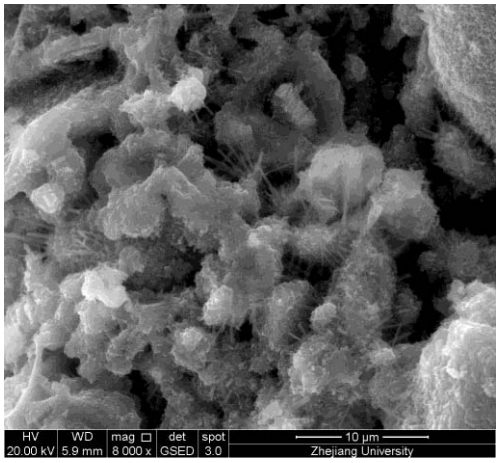

Fig. 3 Microstructural graph of hardened cement paste

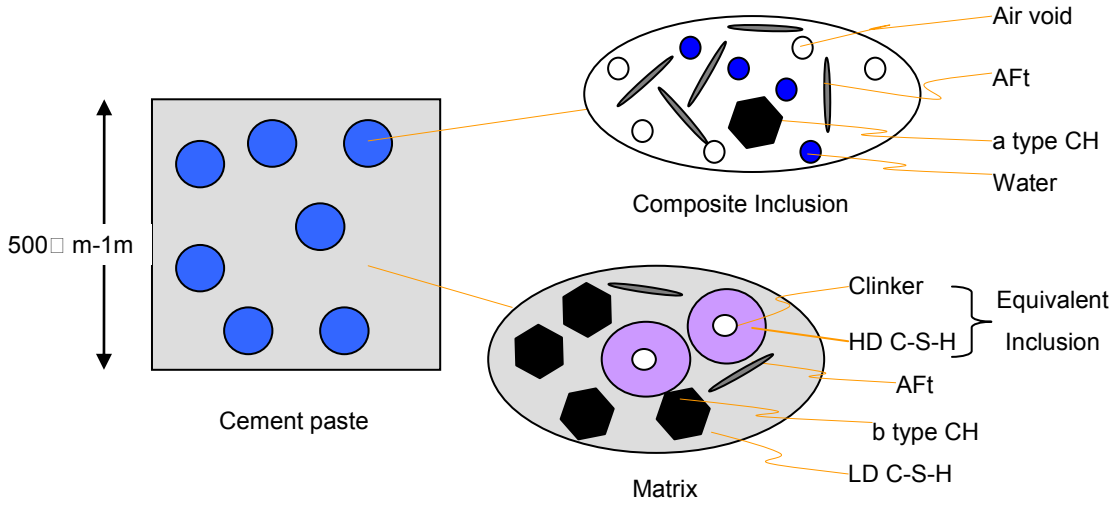

Fig. 4 *Composite-Equivalent Inclusions Model* for hardened cement paste

The flowchart of elasticity prediction of hardened hydrated cement paste by *CEI model* is

(i) Input w/c, hydration degree value and elastic moduli of each individual phase;
(ii) Calculation of volume fractions and elastic stiffness tensors of individual phases according to Eq. (1);

$$f_{clin}(\xi)=\frac{20\times(1-\xi)}{20+63(w/c)},\ f_{water}(\xi)=\frac{63\times[(w/c)-0.42\xi]}{20+63(w/c)},\ f_{air}(\xi)=\frac{3.31\xi}{20+63(w/c)}$$

$$f_{CH}(\xi)=\frac{0.63\times 43.15\xi}{2.29\times[20+63(w/c)]},\quad f_{LD}(\xi)=f'_{LD}(\xi)\times\frac{1.66\times 43.15\xi}{2.29\times[20+63(w/c)]},$$

$$f_{HD}(\xi)=f'_{HD}(\xi)\times\frac{1.66\times 43.15\xi}{2.29\times[20+63(w/c)]} \qquad (1)$$

Where f_{clin}, f_{water}, f_{air}, f_{LD}, f_{HD}, f_{CH} is the volume fractions of clinker, of water, of air, of LD C-S-H, of HD C-S-H, and of CH phases respectively. And f'_{HD}, f'_{LD} is the relative volume fractions of LD C-S-H, of HD C-S-H in total C-S-H, which could be determined by the recommended method in (Tennis and Jennings 2000).

(iii) Calculation of relative volume fractions of individual phases in composite inclusion according to Eq. (2);

$$f_{com} = \sum_{\substack{p=water \\ ,air,CHa}} f_p ,$$

$$f_{water}^{com} = \frac{f_{water}}{f_{com}}, f_{air}^{com} = \frac{f_{air}}{f_{com}}, \quad f_{CHa}^{com} = 1 - f_{water}^{com} - f_{air}^{com} \tag{2}$$

Where f_{water}^{com}, f_{air}^{com}, f_{CHa}^{com} is the relative volume fraction of water phase, of air phase, and of *a* type CH phase respectively;

(iv) Calculation of elastic stiffness tensor of the composite inclusion phase by Eq. (3) based on Self-Consistent scheme;

$$\begin{aligned} C_{com} = & \{ \sum_{p=water,air} f_p^{com} C_p : [I + S_{sph}^{scs} : (C_{com}^{-1} : C_p - I)]^{-1} \\ & + f_{CHa}^{com} C_{CH} : \int_{\phi=0}^{2\pi} \int_{\theta=0}^{\pi} [I + S_{CH}^{scs}(\theta,\phi) : (C_{com}^{-1} : C_{CH} - I)]^{-1} \frac{\sin\theta}{4\pi} d\theta d\phi \} \\ & : \{ \sum_{q=water,air} f_q^{com} [I + S_{sph}^{scs} : (C_{com}^{-1} : C_p - I)]^{-1} \\ & + f_{CHa}^{com} \int_{\phi=0}^{2\pi} \int_{\theta=0}^{\pi} [I + S_{CH}^{scs}(\theta,\phi) : (C_{com}^{-1} : C_{CH} - I)]^{-1} \frac{\sin\theta}{4\pi} d\theta d\phi \}^{-1} \end{aligned} \tag{3}$$

Where C_{com}, C_p, C_q, C_{CH} is the fourth-order elastic stiffness tensor for composite inclusion phase, *p* phase, *q* phase and CH phase, respectively; S_{sph}^{scs} is the fourth-order Eshelby tensor of a spherical inclusion in self-consistent scheme; $S_{CH}^{scs}(\theta,\phi)$ is the fourth-order Eshelby tensor of microCH phase, which equals the Eshelby tensor of an oblate spheroid (with the aspect ratio of 0.7 (Stora et al. 2008) and with axis-orientation defined by the Euler angles) in self-consistent scheme; *I* is the symmetric fourth-order unity tensor.

(v) Calculation of relative volume fractions of individual phases in the equivalent inclusion according to Eq. (4);

$$f_{EI} = \sum_{\substack{p=clin \\ ,HD}} f_p ,$$

$$f_{clin}^{EI} = \frac{f_{clin}}{f_{EI}}, \quad f_{HD}^{EI} = \frac{f_{HD}}{f_{EI}} \tag{4}$$

Where f_{EI} is the total volume fraction of equivalent inclusion phase, f_{clin}^{EI}, f_{HD}^{EI} is the relative volume fraction of unhydrated clinker, and of HD C-S-H in the equivalent inclusion respectively.

(vi) Calculation of elastic stiffness tensor of the equivalent inclusion phase by Eq. (5) based on Mori-Tanaka method;

$$C_{EI}=\{\sum_{\substack{p=clin,\\HD}} f_p^{EI} C_p : [I + S_p^{MT} : (C_{HD}^{-1} : C_p - I)]^{-1}\} : \{\sum_{\substack{q=clin,\\HD}} f_q^{EI} [I + S_q^{MT} : (C_{HD}^{-1} : C_q - I)]^{-1}\}^{-1} \quad (5)$$

Where C_{EI}, C_p, C_q, C_{HD} is the fourth-order elastic stiffness tensor for the equivalent inclusion, clinker and HD C-S-H respectively; S_{clin}^{MT} is the fourth-order Eshelby tensor of clinker, which equals the Eshelby tensor of an oblate spheroid (with the aspect ratio of 0.81 (Stora et al. 2008) and with axis pointing in x_3-direction) in Mori-Tanaka scheme,

(vii) Calculation of elastic stiffness tensor of hardened cement paste by Eq. (6) based on Mori-Tanaka method.

$$\begin{aligned}
C_{CP}=&\{f_{LD}C_{LD}+f_{com}C_{com}:[I+S_{sph}^{MT}:(C_{LD}^{-1}:C_{com}-I)]^{-1}\\
&+f_{EI}C_{EI}:\int_{\phi=0}^{2\pi}\int_{\theta=0}^{\pi}[I+S_{EI}^{MT}(\theta,\phi):(C_{LD}^{-1}:C_{EI}-I)]^{-1}\frac{\sin\theta}{4\pi}d\theta d\phi\\
&+f_{CHb}C_{CH}:\int_{\phi=0}^{2\pi}\int_{\theta=0}^{\pi}[I+S_{CH}^{MT}(\theta,\phi):(C_{LD}^{-1}:C_{CH}-I)]^{-1}\frac{\sin\theta}{4\pi}d\theta d\phi\}\\
&:\{f_{LD}I+f_{com}[I+S_{sph}^{MT}:(C_{LD}^{-1}:C_{com}-I)]^{-1}\\
&+f_{EI}\int_{\phi=0}^{2\pi}\int_{\theta=0}^{\pi}[I+S_{EI}^{MT}(\theta,\phi):(C_{LD}^{-1}:C_{EI}-I)]^{-1}\frac{\sin\theta}{4\pi}d\theta d\phi\\
&+f_{CHb}\int_{\phi=0}^{2\pi}\int_{\theta=0}^{\pi}[I+S_{CH}^{MT}(\theta,\phi):(C_{LD}^{-1}:C_{CH}-I)]^{-1}\frac{\sin\theta}{4\pi}d\theta d\phi\}^{-1}
\end{aligned} \quad (6)$$

Where C_{CP} is the fourth-order elastic stiffness tensor for hardened cement paste; S_{sph}^{MT} is the fourth-order Eshelby tensor of a spherical inclusion in Mori-Tanaka scheme; $S_{EI}^{MT}(\theta,\phi)$ is the fourth-order Eshelby tensor of the equivalent inclusion in LD C-S-H matrix, which equals the Eshelby tensor of an oblate spheroid (with the aspect ratio of 0.7 and with axis-orientation defined by the Euler angles) in Mori-Tanaka scheme.

Assuming the relative volume fraction of *a* type CH in total CH increased from 0 to 1 in *n* order power correlation with w/c increased from 0.55 to 0.9 (porosity increasing from 0.21 to 0.44 in this case) (Eq. (7)), it was found that *n* might lie between 1 and 2 for hardened cement paste with w/c above 0.5 (Fig. 5). By setting *n* as a constant of 1.5, the *CEI Model* accurately predicted the elasticity value of hardened cement paste with w/c ranging from 0.5 to 0.9 with an average error less than 4.3% (Fig. 6), which greatly improved the elasticity prediction accuracy of previous matrix-inclusion type and polycrystalline type RVEs.

$$\frac{f_{CHa}(\xi)}{f_{CH}(\xi)} = 18.9\left(\frac{49.77(w/c) - 23.15\xi - 4.2}{20 + 63(w/c)}\right)^{n} \tag{7}$$

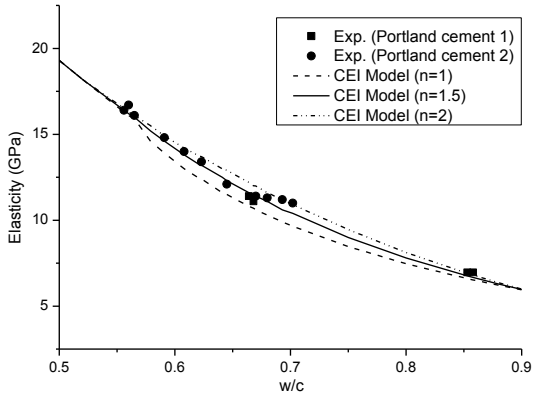

Fig. 5 Verification of *CEI Model* with different *n* values

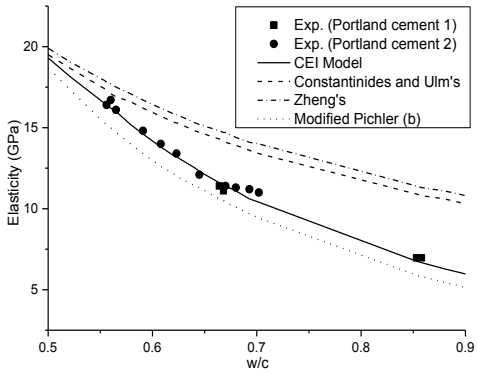

Fig. 6 Predictions of *CEI Model* for fully hydrated cement paste with w/c above 0.5

4. Discussion and Conclusions

This paper provided an insight into the imperfect bonding effect between inclusions and matrix in hardened cement paste, which was seriously ignored in previous application of micromechanics in cement-based materials. It seems the newly proposed RVE (*CEI Model*) was more close to the real nature of cement paste. It improved the prediction accuracy by modeling parts of the inclusions as local polycrystalline composite. This approach may also be applied in mortar and concrete, where the weak interfacial zone between paste and aggregates would have a notable effect in the material's mechanical performance.

The main conclusions of this paper can be drawn as follows:

1. Matrix-inclusion type RVE might overestimate or underestimate the elasticity value of hardened cement paste when w/c was above 0.5 or below 0.4. Polycrystalline type RVE excelled matrix-inclusion type RVE for hardened cement paste with w/c lower

than 0.4.

2. Morphological effect of inclusions had a negligible influence on prediction results when solid volume fraction of harden cement paste was greater than about 79%.
3. By taking the imperfect bonding effect between inclusions and matrix into consideration, the newly proposed *CEI model* could accurately predict the elasticity value of hardened cement paste with w/c ranging from 0.5 to 0.9 with an average error less than 4.3%.

References

Acker, P. (2001). "Micromechanical analysis of creep and shrinkage mechanisms." *Creep, shrinkage, and durability mechanics of concrete and other quasi-brittle materials—Proc., 6th Int. Conf. CONCREEP6@MIT*, F.-J. Ulm, Z. Bazant, and F. Wittmann, eds. Elsevier, Amsterdam, 15-26.

Bernard, O., Ulm, F.-J., and Lemarchand, E. (2003). "A multiscale micromechanics-hydration model for the early-age elastic properties of cement-based materials." *Cem. Concr. Res.*, 33(9), 1293–1309.

Constantinides, G., and Ulm, F.-J. (2004). "The effect of two types of C-S-H on the elasticity of cement-based materials: Results from nanoindentation and micromechanical modelling." *Cem. Concr. Res.*, 34(1), 67–80.

Constantinides, G., and Ulm, F.-J. (2007). "The nanogranular nature of C-S-H." *J. Mech. Phys. Solids*, 55(1), 64–90.

Diamond, S. (2004). "The microstructure of cement paste and concrete—a visual primer." *Cem. Concr. Compos.*, 26(8), 919–933.

Garrault, S., Finot, E., Lesniewska, E., Nonat, A. (2005). "Study of C-S-H growth on C_3S surface during its early hydration.." *Mater. Struct.*, 38(5), 435–442.

Monteiro, P. J. M., and Chang, C. T. (1995). "The elastic moduli of calcium hydroxide." *Cem. Concr. Res.*, 25(8), 1605–1609.

Pichler, B., Hellmich C., Eberhardsteiner J. (2009). "Spherical and acicular representation of hydrates in a micromechanical model for cement paste: prediction of early-age elasticity and strength", *Acta Mechanica*, 203(3-4), 137–162.

Pichler, B., and Hellmich, C. (2011). "Upscaling quasi-brittle strength of cement paste and mortar: A multi-scale engineering mechanics model." *Cem. Concr. Res.*, 41(5), 467–476.

Scrivener, K.L. (2004). "Backscattered electron imaging of cementitious microstructures: understanding and quantification." *Cem. Concr. Res.*, 26(6), 935–945.

Stora, E., He, Q.-C., Bary, B. (2006). "Influence of inclusion shapes on the effective linear elastic properties of hardened cement pastes." *Cem. Concr. Res.*, 36(10), 1330–1344.

Tennis, P. D., and Jennings, H. M. (2000). "A model for two types of C-S-H in the microstructure of cement paste." *Cem. Concr. Res.*, 30(6), 855–863.

Zheng, J., Zhou, X., Shao, L., and Jin, X. (2010). "Simple three-step analytical scheme for prediction of elastic moduli of hardened cement paste." *J. Mat. Civ. Eng. (ASCE)*, 22(11), 1191–1194.